Cell Host & Microbe
Article

A Type III Secretion System in *Vibrio cholerae* Translocates a Formin/Spire Hybrid-like Actin Nucleator to Promote Intestinal Colonization

Vincent C. Tam,[1] Davide Serruto,[1,4] Michelle Dziejman,[3] William Brieher,[2] and John J. Mekalanos[1,*]
[1] Department of Microbiology and Molecular Genetics
[2] Department of Systems Biology
Harvard Medical School, 200 Longwood Avenue, Boston, MA 02115, USA
[3] Department of Microbiology and Immunology, University of Rochester School of Medicine and Dentistry, 601 Elmwood Avenue, Rochester, NY 14642, USA
[4] Present address: Novartis Vaccines, Via Fiorentina 1, 53100 Siena, Italy.
*Correspondence: john_mekalanos@hms.harvard.edu
DOI 10.1016/j.chom.2007.03.005

SUMMARY

We have previously characterized a non-O1, non-O139 *Vibrio cholerae* strain, AM-19226, that lacks the known virulence factors but contains components of a type III secretion system (T3SS). In this study, we demonstrated that the T3SS is functional and is required for intestinal colonization in the infant mouse model. We also identified VopF, which is conserved among T3SS-positive *V. cholerae* strains, as an effector containing both formin homology 1-like (FH1-like) and WASP homology 2 (WH2) domains. Translocation of VopF by *V. cholerae* or expression by transfection altered the actin cytoskeletal organization of the eukaryotic host cells. In vitro domain analysis indicated that both FH1-like and WH2 domains are required for actin nucleation and polymerization activity. These data correlate with in vivo data, suggesting that VopF-mediated alteration of actin polymerization homeostasis is required for efficient intestinal colonization by T3SS+ *V. cholerae* in the infant mouse model.

INTRODUCTION

Vibrio cholerae is a Gram-negative, facultative pathogen that causes the diarrheal disease cholera. Recent history has recorded seven pandemics of cholera caused by strains of two serogroups, O1 and O139. The common virulence mechanism of these strains is well characterized and depends on elaboration of the toxin coregulated pilus (TCP) and cholera toxin (CT) (Faruque et al., 1998). TCP is a type IV pilus that is thought to play a role in adherence in human infection and is required for colonization of the small intestine in the infant mouse model (Thelin and Taylor, 1996). CT is an AB toxin that causes disruption in CFTR ion channel homeostasis, leading to watery diarrhea (Faruque et al., 1998). While O1 and O139 strains continue to cause endemic, epidemic, and pandemic disease, non-O1, non-O139 strains embody a genetically diverse group of strains that can cause outbreaks and sporadic disease in a TCP- and CT-independent manner using undefined virulence mechanisms. Although these strains rarely cause pandemic disease, they represent an emerging threat and are of increasing concern in endemic areas and worldwide (Faruque et al., 2004).

Previously, we characterized a non-O1, non-O139 clinical isolate from Bangladesh, AM-19226, which colonized infant mice and was pathogenic for rabbits despite the fact that the genes encoding TCP and CT were absent (Dziejman et al., 2005). Microarray and hybridization analyses showed that the strain lacked genes encoding TCP and CT in addition to ~200 other genes when compared to the pandemic O1 El Tor strain N16961. Sequencing of random fragments library revealed an ~30 kb contig having >90% nucleic acid identity to one of the type III secretion systems (T3SS2) of pandemic *Vibrio parahaemolyticus*. A type III secretion system (T3SS) is a specialized secretion apparatus utilized by Gram-negative pathogens to translocate virulence factors, or effector proteins, into host cells where they function to alter the eukaryotic cellular machinery (Galan and Collmer, 1999; Hueck, 1998). T3SS have been associated with pathogenic mechanisms in a wide variety of bacteria including *Pseudomonas*, *Salmonella*, *Yersinia*, and *Shigella* but until now have not been described for *V. cholerae*.

One common function of some T3SS effectors is reorganization of the host actin cytoskeleton to benefit the pathogen. Frequently, this is achieved by mimicking the function of a eukaryotic protein (Galan and Collmer, 1999; Galan and Wolf-Watz, 2006): examples include Yops from *Yersinia*, Sops and Sips from *Salmonella* (Rottner et al., 2005), and Tir from enteropathogenic or enterohemorrhagic *E. coli* (EPEC/ EHEC) (Campellone et al., 2002; Goosney et al., 2001). In eukaryotic cells, there are three families of proteins involved in the nucleation of actin: Arp2/3, Spire, and formin. The Arp2/3 complex, when activated, forms branched actin filaments (Welch et al., 1998). The Spire protein contains a cluster of four WH2 domains, which bind and nucleate actin (Quinlan

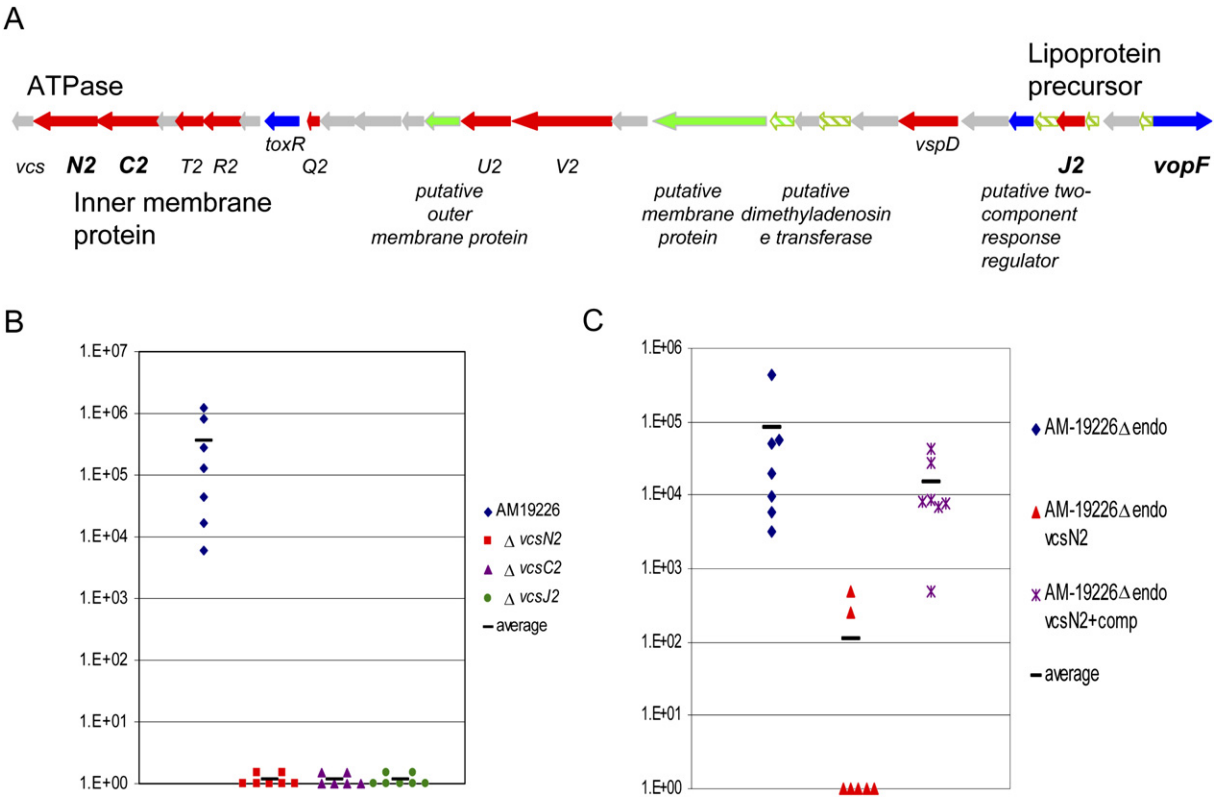

Figure 1. T3SS Is Required for Colonization in the Infant Mouse Model

(A) Genetic organization of T3SS contig 247 in AM-19226 (Dziejman et al., 2005). Genes indicated in bold were targeted for deletion.

(B) Single-strain colonization of infant mouse small intestine. Deletion mutants of structural genes *vcsN2*, *vcsC2*, and *vcsJ2*, and wild-type AM-19226 were inoculated into 5-day-old infant mice. CFU recovered 20 hr postinfection from the small intestine are shown in log scale on the y axis.

(C) Single-strain colonization of MD992 (AM-19226 Δ*endo*), VTV19 (AM-19226 Δ*endo vcsN2*), and VTV19 pVTM24 (AM-19226 Δ*endo vcsN2 vcsN2*::pBBR1MCS4).

et al., 2005). Finally, formins, which contain FH1 and FH2 domains, form unbranched actin cables within cells (Faix and Grosse, 2006). Both the Arp2/3 complex and Spire bind the pointed end of actin filaments, unlike formins, which interact with the fast-growing barbed end (Kovar et al., 2003; Pruyne et al., 2002). While some bacterial pathogens, including *Listeria* and *Shigella*, express virulence factors exploiting the Arp2/3 complex to facilitate motility within host cells (Cossart, 2000; Goldberg, 2001), molecular mimicry of Spire and formin nucleation activity have not been identified in any bacteria. Recently, *Chlamydial* TARP protein has been shown to nucleate actin by a mechanism distinct from other known nucleators utilizing only a single WH2 domain (Jewett et al., 2006). Here we show that an essential virulence effector protein of T3SS$^+$ *V. cholerae* is a molecular mimic of formin, and to some extent Spire, that can alter actin polymerization in vitro and in vivo.

RESULTS

T3SS Is Required for Virulence in the Infant Mouse Model

Because AM-19226 does not contain the canonical virulence factors TCP and CT, we wanted to examine whether T3SS could provide an alternate colonization mechanism in the infant mouse model. Deletion of the putative structural genes *vcsN2* (ATPase), *vcsC2* (inner membrane protein), or *vcsJ2* (lipoprotein) (Figure 1A) produced a five-log defect in colonization of the infant mouse model when compared to wild-type AM-19226 (Figure 1B). Our initial mutant characterization was conducted using marker-exchanged mutants because AM-19226 contains a restriction modification system (M.D., unpublished data) that hinders genetic manipulation using suicide vectors. A restriction endonuclease was identified and deleted from AM-19226, creating strain MD992, which allows standard genetic manipulation (M.D, unpublished data). An in-frame, nonpolar deletion of *vcsN2* was constructed in MD992, and the mutant failed to colonize the infant mouse small intestine. This colonization defect was complemented to within one log of MD992 by providing *vcsN2* in *trans*, carried by pBBRMCS-4 (Kovach et al., 1995), a broad-host-range plasmid with a constitutive promoter (Figure 1C). The incomplete complementation may be due to the instability of the plasmid in the absence of antibiotic selection in vivo. We observed a loss of plasmid antibiotic marker in colonies recovered from the small intestine (data not shown). The colonization defect of the

structural gene mutants and the *vcsN2* complementation experiment suggest that a functional T3SS is required for AM-19226 colonization in the infant mouse model.

Domain Organization and Conservation of VopF, a Predicted Protein Containing FH1-like/WH2 Domains

In many type III secretion systems, genes encoding effector proteins can be found embedded in T3SS pathogenicity islands. A gene annotated as NT01VC2350 and located within the *V. cholerae* T3SS pathogenicity island is predicted to encode a protein of 530 aa, containing one proline-rich sequence that resembles a formin homology 1 (FH1) domain and three WASP homology 2 (WH2) domains (PFam; Dziejman et al., 2005) (Figure 2A). These domains have been associated with eukaryotic actin-binding proteins. The presence of eukaryotic protein domains marks NT01VC2350 as a candidate effector that might interact with host actin, and we have named this gene *vibrio outer protein F* (*vopF*). The predicted product of NT01VC2350, VopF is quite similar to its ortholog in *V. parahaemolyticus* (Vpa1370), having 57% identical residues and 71% positive matches at the amino acid level. There are also subtle differences between the two proteins, including a deletion from aa 66 to 95 in Vpa1370 and a smaller deletion in the FH1-like domain compared to VopF (Figure 2B).

FH1 is a hypervariable domain that ranges in size from 15 to 229 residues and has a high proline content of 35%–100% (Higgs, 2005; Kitayama and Uyeda, 2003; Rivero et al., 2005). FH1 is a binding site for profilin, which binds actin monomers and prevents spontaneous nucleation. A protein sequence alignment of the VopF FH1-like domain to other FH1 domain proteins and their respective E values from domain searches is provided in Figure 2C. Interestingly, Vpa1370 did not yield any significant matches to the FH1 domain.

While most formin proteins contain FH1 and FH2 domains, VopF lacks an FH2 domain and instead contains three WH2 domains downstream of the FH1-like domain. A WH2 domain is a small motif found in many different regulators of the actin cytoskeleton and has been shown to bind actin monomers (Paunola et al., 2002). A protein sequence alignment of the VopF WH2 domains to other WH2 domains is provided in Figure 2D. Spire, which is a novel actin nucleator distinct from Arp2/3 and formins, contains four WH2 domains and nucleates actin by binding actin monomers. A critical and conserved linker region between the third and fourth WH2 domains within Spire is required for sufficient actin nucleation (Quinlan et al., 2005). While no similar linker sequence exists in VopF, a proline-rich motif is present between the second and third WH2 domains (Figure 2A). This seven-amino acid motif could be a cryptic binding site for profilin, which has weak affinity to as few as six poly (L-proline) residues (Petrella et al., 1996). The domain structure of VopF suggests that it is likely to interact with the host actin cytoskeleton.

To determine whether VopF is conserved among *V. cholerae* non-O1, non-O139 strains, we performed a Southern analysis surveying 38 clinical and environmental isolates (Figure 3). Using probes that hybridize to the structural components *vcsN2* and *vcsC2*, and to the putative effector *vopF*, we determined that all strains that were T3SS positive (15/38) also contained *vopF* (15/15). The domain structure and conservation of *vopF* suggested that it is a putative effector for the *V. cholerae* T3SS.

Translocation of *V. cholerae* T3SS Effector Protein VopF

To determine whether *vopF* from AM-19226 encodes a type III effector that is translocated directly from the bacterial cytoplasm into the host cytosol, we used a TEM β-lactamase fusion as a reporter for translocation (Charpentier and Oswald, 2004). In the translocation assay, eukaryotic host cells take up and esterify a substrate (CCF2/AM) with two fluorophores, causing them to emit green fluorescence due to fluorescent resonant energy transfer (FRET). When translocated into host cells, β-lactamase fusion proteins cleave the substrate, thus disrupting FRET and resulting in cells that emit blue fluorescence. To use *V. cholerae* in the tissue-culture model, we made in-frame deletions in *rtxA*, *hlyA*, and *hapA* in MD992; these genes encode accessory toxins that are cytotoxic to eukaryotic cells (Fullner et al., 2002). The resulting strain (VTV18) was used in all further tissue culture experiments. In order to perform the translocation assay, we fused both full-length *vopF* (aa 1–530) and an N-terminal fragment (aa 1–100) to β-lactamase. As a positive control we used a β-lactamase fusion to full-length *vpa1346* or *vopP*, a *Yersinia* YopP homolog found in *V. parahaemolyticus* that has been shown to be secreted by T3SS2 (Park et al., 2004) but that has not been identified in AM-19226. Western blotting of protein samples from the translocation assays confirmed that all proteins were expressed equally (Figure 4A). Cells infected with VTV18 expressing VopF or Vpa1346 fusion proteins emitted blue fluorescence, indicating that translocation of the reporters had occurred (Figure 4B). VTV20 (VTV18 Δ*vcsN2*) failed to translocate either of the fusion proteins, demonstrating that the translocation process is type III dependent. Further, since the β-lactamase fusion protein with VopF aa 1–100 was translocated when expressed in VTV18, we determined that the secretion and translocation signals are located in the amino terminus of the protein as has been shown for all T3SS effectors. These data suggest *vopF* encodes a potential effector protein of the *V. cholerae* T3SS system, since its translocation to eukaryotic host cells is dependent on a functional T3SS.

Infection with AM-19226 or Transfection of VopF Induces Actin-Rich Filoform Formation in Tissue Culture Cells

Since VopF contains domains homologous to both formin and Spire, we next wanted to examine how AM-19226 interacts with human epithelial cells in vitro and whether the strain has the capacity to disrupt host cell actin cytoskeletal organization. We infected the human epithelial cell line HEp-2 with VTV18, incubated it with anti-AM-19226 antibody and fluorescent stains, and examined the cells

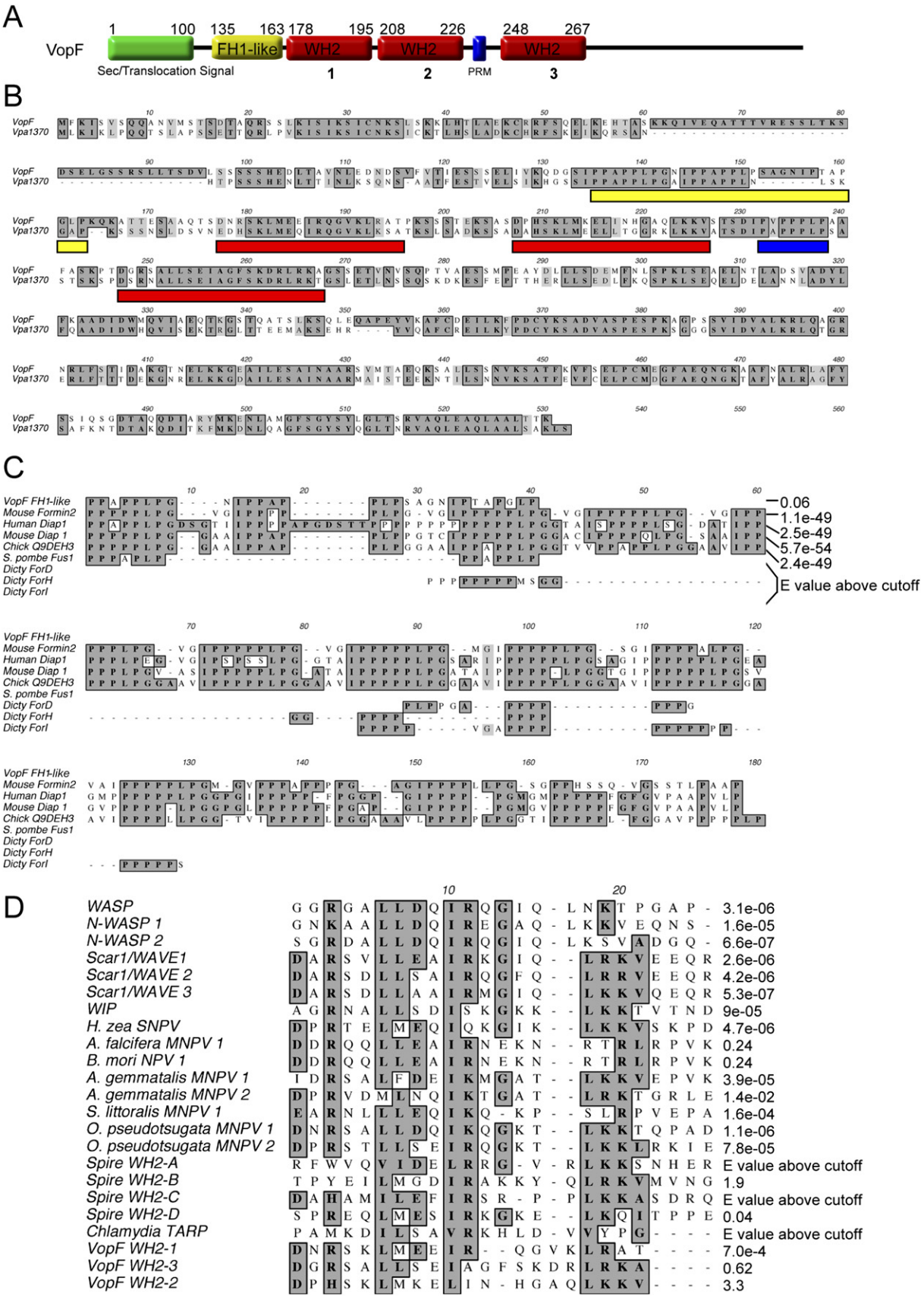
A
VopF
1
100
135
163
178
195
208
226
248
267
FH1-like
WH2
WH2
WH2
Sec/Translocation Signal
1
2
PRM
3
B
VopF
Vpa1370
C
VopF FH1-like
Mouse Formin2
Human Diap1
Mouse Diap 1
Chick Q9DEH3
S. pombe Fus1
Dicty ForD
Dicty ForH
Dicty ForI
0.06
1.1e-49
2.5e-49
5.7e-54
2.4e-49
E value above cutoff
D
WASP 3.1e-06
N-WASP 1 1.6e-05
N-WASP 2 6.6e-07
Scar1/WAVE1 2.6e-06
Scar1/WAVE 2 4.2e-06
Scar1/WAVE 3 5.3e-07
WIP 9e-05
H. zea SNPV 4.7e-06
A. falcifera MNPV 1 0.24
B. mori NPV 1 0.24
A. gemmatalis MNPV 1 3.9e-05
A. gemmatalis MNPV 2 1.4e-02
S. littoralis MNPV 1 1.6e-04
O. pseudotsugata MNPV 1 1.1e-06
O. pseudotsugata MNPV 2 7.8e-05
Spire WH2-A E value above cutoff
Spire WH2-B 1.9
Spire WH2-C E value above cutoff
Spire WH2-D 0.04
Chlamydia TARP E value above cutoff
VopF WH2-1 7.0e-4
VopF WH2-3 0.62
VopF WH2-2 3.3

using fluorescent microscopy. Infection of HEp-2 cells with VTV18 expressing wild-type VopF caused the formation of aberrant protrusions from the periphery as well as the appearance of an increased amount of actin-rich filoform on the surface and periphery of the cells (Figure 5A). We constructed a mutant in VTV18 with an in-frame deletion of *vopF* (*ΔvopF*) and another mutant with a deletion of the FH1-like and all three WH2 domains within *vopF* (Dm2) (Figure 7A). HEp-2 cells infected with the Δ*vopF* or Dm2 mutant remained relatively smooth around the surface, and no noticeable protrusions were observed (Figure 5A). We quantified the number and length of protrusions in cells infected with VTV18, VTV20 (Δ*vcsN2*), VTV29 (Δ*vopF*), and VTV33 (ΔDm2) (Figure 5B). Cells infected with VTV18 exhibited more protrusions (43 per cell) and longer protrusions (mean = 4.7 μm) than VTV20 (28.5 protrusions per cell; 2.7 μm), VTV29 (30.3 protrusions per cell; 2.9 μm), and VTV33 (31.2 protrusions per cell; 2.6 μm). The differences between the mean of VTV18 and VTV20, VTV29, and VTV33 are statistically significant using the Student's t test (p values < 0.0001). To localize VopF within infected cells, we stained VopF or Dm2 mutant proteins with polyclonal anti-VopF antibodies and fluorescent stain (Figure 5C). Cells infected with VTV18 showed localization of anti-VopF antibodies at the tip of the protrusions. Cells infected with VTV33 (ΔDm2) had fewer protrusions on the cell periphery, and anti-VopF antibodies did not localize at or near the protrusions. These data suggest that VopF is directly involved in actin-rich filoform formation in infected cells.

T3SS typically translocate multiple effectors into eukaryotic host cells to optimize the success of infection. To study the effect of VopF on host cells in the absence of confounding effects from other translocated proteins, we transfected expression plasmids carrying *vopF* into Chinese hamster ovary (CHO) cells and examined the effects on actin dynamics and cell morphology. We cotransfected a plasmid expressing GFP as a positive control for cells that had taken up the plasmid DNA. Cells transfected with *vopF* showed an explosive formation of protrusions, reminiscent of reported changes resulting from transfection of activated formins or eukaryotic protein regulators that activate formins (Pellegrin and Mellor, 2005; Peng et al., 2003; Schirenbeck et al., 2005) (Figure 6A). This cellular phenotype was absent in cells transfected with GFP alone, GFP and empty vector, or GFP and vector carrying the Dm2 mutant. The infection and transfection experiments together demonstrate that delivery of VopF into host cells alters the actin cytoskeleton and cell morphology in a manner similar to formin.

Based on the evidence presented thus far showing an effect of VopF on the actin cytoskeleton, we decided to determine the nature of the interaction between VopF and actin. To test whether VopF associates with the fast growing barbed end of actin filaments in the actin-rich filoform, as in the case of formin, or localizes at the slow-growing pointed end like Spire, we transfected a *vopF*::*gfp* or Dm2::*gfp* gene fusion into CHO cells. In cells transfected with *vopF::gfp*, an enrichment of VopF-GFP proteins at the tips of the protrusions was observed suggesting that VopF, like formin, is associated with the fast-growing barbed end (Figure 6B) (Pellegrin and Mellor, 2005). In contrast, Dm2-GFP does not localize to a specific site within the host cells. Line scan measurements of pixel intensities along the cell protrusions confirmed the localization of VopF-GFP but not Dm2-GFP at the distal ends of the filoform structures (Figure 6C). Together, these results suggest that VopF mimics formin protein in its association with actin, inducing actin-rich protrusion formation in host cells.

In Vitro Activity of VopF Correlates with In Vivo Colonization

To determine how the various domains of VopF contribute to actin nucleation and polymerization, multiple VopF domain deletion mutants (Dm) were constructed (Figure 7A). Wild-type VopF and mutant proteins were expressed, purified, and examined in the pyrene actin assay for the ability to nucleate and polymerize actin (Figure 7B). Wild-type VopF alone was able to nucleate and polymerize actin in the absence of any cellular components. Its activity was abrogated by the addition of cytochalasin D, which blocks barbed-end polymerization. The nucleating activity of VopF was also dependent on the FH1-like and WH2 domains, since the Dm2 mutant (VopFΔFH1L 3WH2) failed to nucleate actin. Deletion of all three WH2 domains, Dm1 (VopFΔ3WH2), also resulted in a protein unable to nucleate actin. As in the case of Spire (Quinlan

Figure 2. Domain Structure and Sequence Alignments of VopF

Identical amino acids are boxed in dark shadowing; conserved amino acids are indicated by light shadowing. E values of homology searches are listed to the right.

(A) Graphical representation of domain organization in VopF, a 530 aa protein having a formin homology 1-like (FH1-like) domain (aa 135–163) and three WASP homology 2 (WH2) domains: WH2-1 (aa 178–195), WH2-2 (aa 208–226), and WH2-3 (aa 248–267). A proline-rich motif (PRM) exists between the second and third WH2 domain spanning from aa 232 to 238.

(B) Protein sequence alignment between VopF from *V. cholerae* AM-19226 and its ortholog, Vpa1460, in *V. parahaemolyticus* RIMD 2210633. The yellow box highlights the FH1-like domain sequence; red boxes highlight the WH2 domain sequences; the blue box highlights the PRM sequence.

(C) Protein sequence alignment between VopF FH1-like domain with other FH1 domain-containing proteins. Accession numbers: mouse Formin 2, NP_062318; human Diap1, O60610; mouse Diaphanous 1, AAH70412; chick Diaphanous, Q9DEH3; *Schizosaccharomyces pombe* Fus1, AAA99003; *Dictyostelium discoideum* ForminD, XP_640306; ForminH, XP_638143; Formin I, XP_638543.

(D) Protein sequence alignment between VopF WH2 domains and other WH2 domain-containing proteins, partially adapted from Machesky et al. (2001). Accession numbers: WASP, NP_000368; N-WASP 1, BAA20128; N-WASP 2, NP_003932.3; Scar1/WAVE1, Q92558; Scar1/WAVE2, Q9Y6W5; Scar1/WAVE3, AAL51032; WIP, NP_003378; *H. zea* SNPV, AAB54090; *A. californicus* MNPV 1, NP_054038; *B. mori* NPV 1, NP_047415; *A. gemmatalis* MNPV1, *A. gemmatalis* MNPV2, YP_803394; *S. littoralis* MNPV1, CAA68047; *O. pseudotsugata* MNPV, NP_046158; *Drosophila melanogaster* Spire, AAF23615; *Chlamydia trachomatis* TARP, YP_328278.

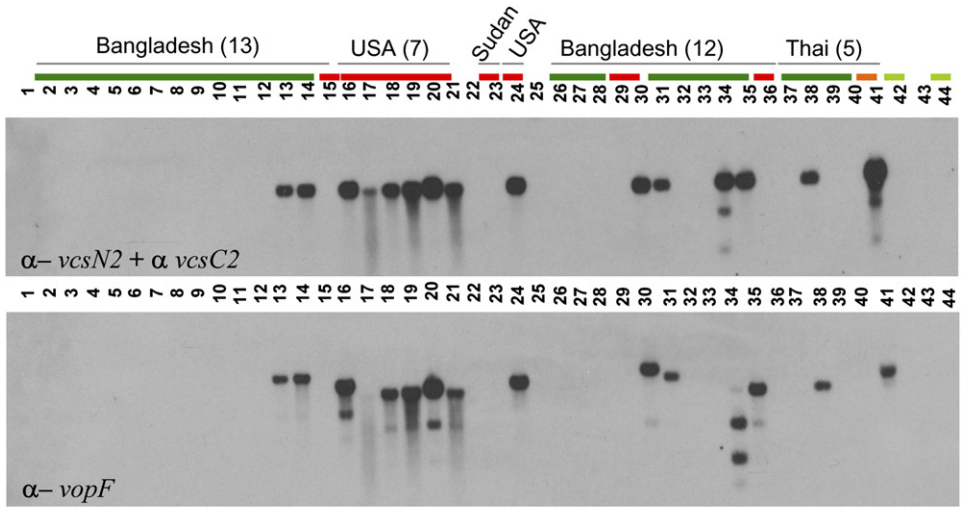

#	Strain	Serogroup	T3SS	vopF	#	Strain	Serogroup	T3SS	vopF
1					23	V52	O37	-	-
2	660V1159	non-O1/O139	-	-	24	V55	O141	+	+
3	707V1236	non-O1/O139	-	-	25				
4	724V1267	non-O1/O139	-	-	26	504-931	O18	-	-
5	871V1469	non-O1/O139	-	-	27	622-37	O23	-	-
6	R-612V29	non-O1/O139	-	-	28	612-29	O37	-	-
7	R-616V33	non-O1/O139	-	-	29	MZO-3	O37	-	-
8	R-641V50	non-O1/O139	-	-	30	AM-19226	O39	+	+
9	R-645V53	non-O1/O139	-	-	31	652-58	O5	+	+
10	624-40	non-O1/O139	-	-	32	871-147	O6	-	-
11	656-59	O10	-	-	33	862-133	O79	-	-
12	523-955	O14	-	-	34	641-49	O8	+	+
13	831-65	O14	+	+	35	842-86	O8	+	+
14	838-77	O14	+	+	36	AM-15622	O8	-	-
15	MZO-2	O14	-	-	37	WBDV-101E	O49	-	-
16	V46	O141	+	+	38	FY-2G	O8	+	+
17	V47	O141	+	+	39	F2DH514	non-O1/O139	-	-
18	V48	O141	+	+	40	PV53-II	non-O1/O139	-	-
19	V49	O141	+	+	41	599B2	non-O1/O139	+	+
20	V50	O141	+	+	42	N16961	O1	-	-
21	V51	O141	+	+	43				
22					44	VP47	V.parahaemolyticus	+	+

Figure 3. Correlation of *vopF* with the Presence of T3SS Structural Components

Forty *Vibrio* strains were included in the Southern analysis: 38 non-O1, non-O139 clinical and environmental strains; N16961, an O1 El Tor biotype; and VP47, a T3SS+ *V. parahaemolyticus* strain. Genomic DNA of each strain was purified, digested with EcoRI, and transferred to a nylon membrane, which was probed using PCR products generated from the AM-19226 ORFs *vcsN2*, *vcsC2*, and *vopF*. The results were summarized in the table; (+) and (–) denote positive or negative hybridization, respectively. Dark green bars denote environmental strains, red bars denote clinical strains, and light green bars denote positive (VP47) and negative (N16961) control. A positive signal from *V. parahaemolyticus* only occurred after longer exposure.

et al., 2005), deletion of individual *vopF* WH2 domains, Dm4, Dm5, and Dm6, still allowed sufficient nucleation of actin monomer, though at a slower rate compared to wild-type VopF. Dm3 (VopFΔFH1L) retained some nucleation activity, presumably by binding monomeric actin with the three intact WH2 domains similarly to Spire protein, which nucleates actin with four WH2 domains. We determined that the lower steady state was not a result of fluorescence quenching or light scattering by the mutant protein (data not shown). Whether Dm3 protein failed to polymerize actin and affected the critical concentration of actin require further experimentation to address the biophysical properties of VopF-dependent actin polymerization.

To understand how the in vitro activity of VopF translates to in vivo effects on colonization, we examined the ability of various in-frame *vopF* deletions in AM-19226 to directly compete with wild-type AM-19226 in the colonization model. We found that the ability to nucleate actin directly correlates with the ability to colonize the infant mouse small intestine (Figure 7C). AM-19226 Δ*vopF*, Dm1, and Dm2 mutants, which contain no actin nucleation or polymerization activity, each displayed a 1.5 log defect in colonization compared to the wild-type strain. The Dm3 mutant had limited nucleation activity (Figure 7B) but failed to colonize efficiently, suggesting that the FH1-like domain is required for VopF to function efficiently in vivo. This property is similar to the formin protein, which requires

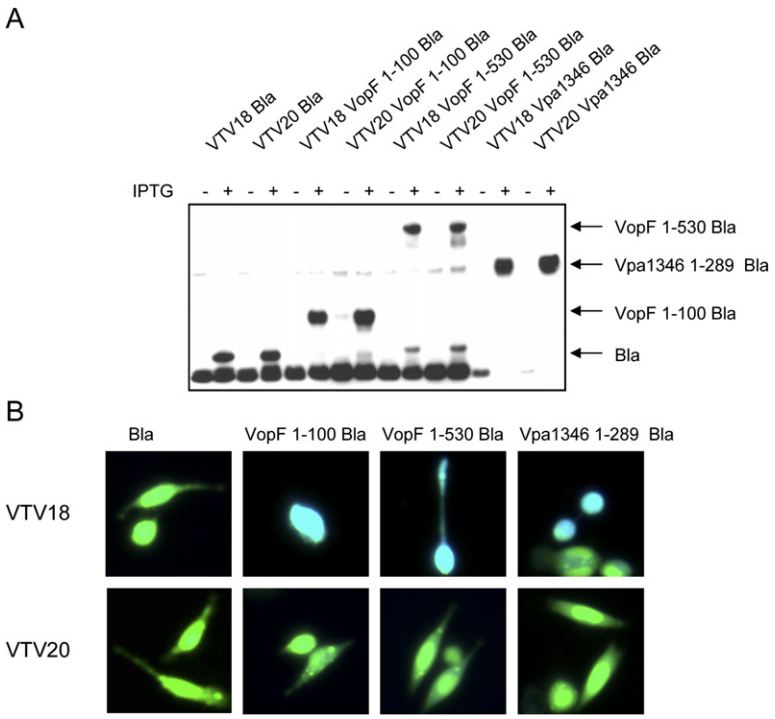

Figure 4. VopF Translocation into Host Cell Is T3SS Dependent

(A) VTV18 (AM-19226 Δ*endo rtxA hlyA hapA*) and VTV20 (AM-19226 Δ*endo rtxA hlyA hapA vcsN2*) carrying IPTG-inducible β-lactamase fusions to WT *vopF*, *vopF* encoding aa 1–100, or *vpa1346*. Cell lysates of bacteria expressing various fusion proteins were resolved by 4%–12% SDS/PAGE and subjected to immunoblotting with a β-lactamase-specific antibody.

(B) HEp-2 cells were infected with VTV18 or VTV20 expressing β-lactamase fusion proteins described in (A). After infection, HEp-2 cells were loaded with CCF2/AM substrate, which can be cleaved by translocated β-lactamase fusion proteins, resulting in HEp-2 cells that emit blue fluorescence. Cells with uncleaved substrate emit green fluorescence.

FH1 domain for in vivo function and polymerization of actin filaments in the presence of profilin (Evangelista et al., 2002; Moseley et al., 2004). Dm4, Dm5, and Dm6 mutants, which have actin nucleation and polymerization activities in vitro, were able to colonize in vivo comparable to wild-type. These results confirm the physiological relevance of VopF in vitro activity and suggest that VopF activity is essential for AM-19226 virulence.

DISCUSSION

Many bacterial pathogens affect actin homeostasis in host cells, and these alterations play important roles in their virulence mechanisms (Stevens et al., 2006). For example, ActA from *Listeria* (Smith and Portnoy, 1997) and IcsA from *Shigella* (Goldberg and Theriot, 1995) activate Arp2/3 complex either directly or via N-WASP to gain motility intracellularly, while the Tir protein from EPEC or EHEC activates Arp2/3 complex to form actin-rich pedestals (Campellone et al., 2002; Goosney et al., 2001). Invasive pathogens have also employed actin-dependent cellular processes for internalization into eukaryotic host cells (Collazo and Galan, 1997; Cossart, 1997; Isberg and Van Nhieu, 1994). Here we show that VopF, an effector protein from *V. cholerae* AM-19226, nucleates actin and is required for in vivo colonization of AM-19226 in competition assays with VopF deletion mutants. In vitro infection and transfection experiments demonstrate that VopF alters the actin dynamics and cell morphology of host cells, causing surface protrusion formation. One can speculate how these surface structures could serve to disperse the bacteria onto neighboring intestinal cell surfaces and thus promote efficient colonization.

We currently do not understand how expression of VopF promotes intestinal colonization of *V. cholerae*. Because VopF deletion mutants have colonization defects in competition assays with wild-type AM-19226, we hypothesize that VopF exerts a localized effect on host cells. This restricted action benefits only the bacterial cells that express and translocate VopF, and not "bystander" vibrios that are T3SS competent but do not express a functional VopF. This is an important distinction because virulence factors like cholera toxin stimulate colonization of wild-type vibrios in mono infection but can also rescue the colonization defect of CTX− mutants in competition assays (Pierce et al., 1985; Peterson and Mekalanos, 1988). Thus, VopF is not likely to produce a diffusible effect such as one might expect for a diffusible toxin or diffusible host response (e.g., growth stimulation in the intestine by inducing diarrhea). Rather, VopF will likely stimulate intestinal colonization by an in situ effect such as killing host immune effectors cells that have phagocytosed vibrios (e.g., macrophages and neutrophils). Alterations of actin homeostasis have been shown to have a cytotoxic effect on host cells (Popoff, 1998). For example, toxins such as RtxA of *V. cholerae* (Fullner and Mekalanos, 2000), the cytolethal distending toxins of various bacterial organisms (Aragon et al., 1997), and various other T3SS effector proteins (Lerm et al., 2000; Fiorentini et al., 2003) disrupt actin homeostasis and as a result directly kill cells. Thus, VopF may have a specific localized cytotoxic effect on intestinal epithelial or inflammatory cells. Alternatively, VopF may alter the actin cytoskeleton of neutrophils to evade the innate immune response.

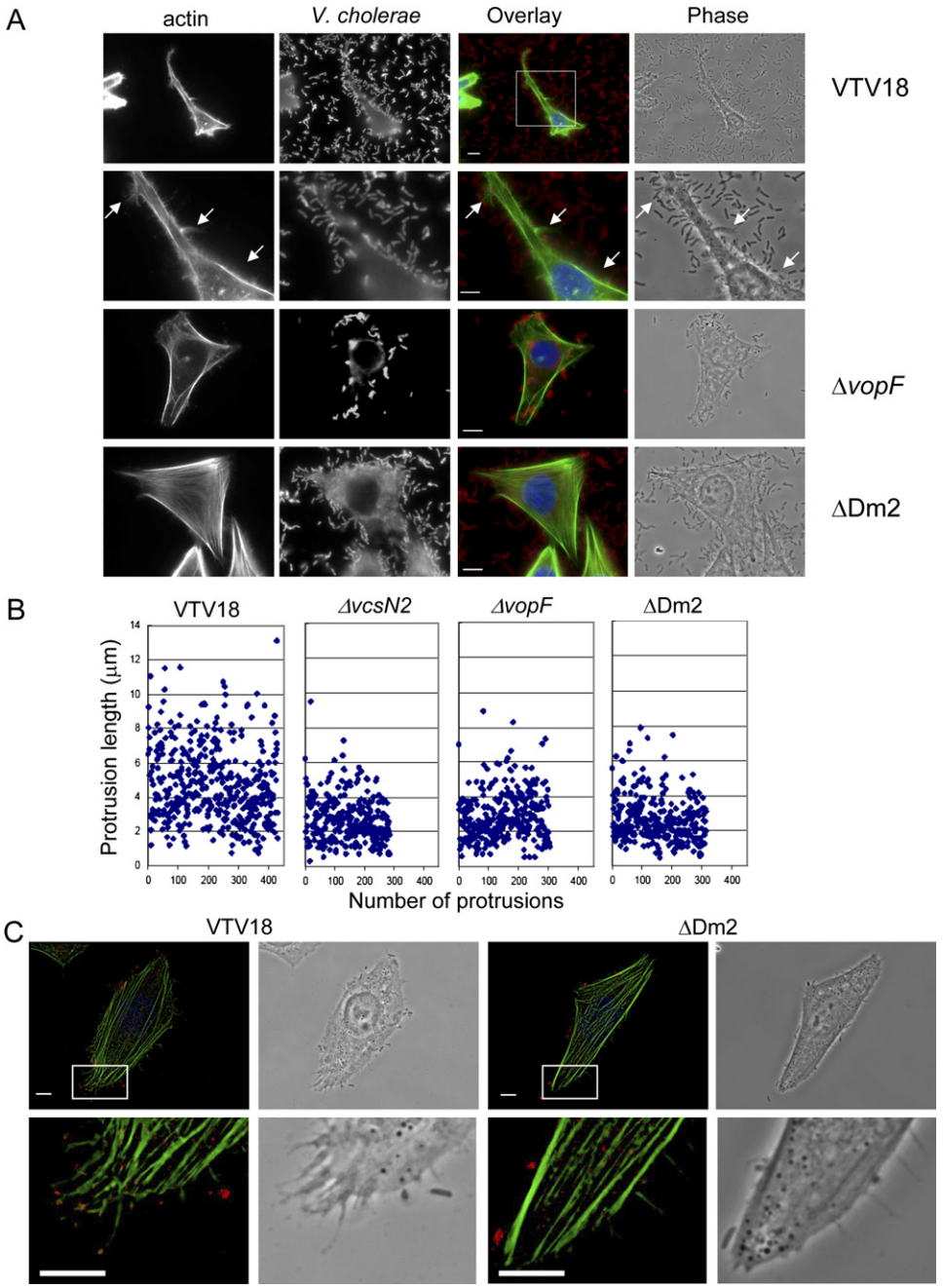

Figure 5. Delivery of VopF by Infection Induces Actin-Rich Filoform Formation in Tissue Culture Cells

(A) HEp-2 cells were infected with *V. cholerae* VTV18 (AM-19226 Δ*endo rtx hly hap*), VTV29 (AM-19226 Δ*endo rtx hly hap vopF*), and VTV33 (AM-19226 Δ*endo rtx hly hap* Dm2). Cells were fixed with 3.7% formaldehyde and permeabilized with 0.1% Triton X-100. Actin was stained with Alexa Fluor 488 phalloidin (green), bacteria were stained with anti-AM-19226 antibodies and Alexa Fluor 568 anti-rabbit antibodies (red), and nucleus was stained with DAPI (cyan). Cells were also visualized with phase contrast light microscopy. Second row is a higher magnification of the boxed area. White arrows point to the aberrant protrusions on the periphery of the cell.

(B) Quantification of protrusions on cell infected with VTV18, VTV20 (AM-19226 Δ*endo rtx hly hap vcsN2*), VTV29, and VTV33. Forty infected cells (ten in each group) were counted for the number and length of the protrusions. Data were plotted with x axis as the number of protrusions and y axis as the length of that particular protrusion.

(C) HEp-2 cells were infected and stained as in (A) with the exception that the VopF or Dm2 mutant proteins were stained with anti-VopF antibodies. Micrographs were processed for 2D deconvolution (Metamorph, Molecular Devices). Overlay images of actin (green), VopF (red), and DAPI (cyan) stains and phase contrast images were shown. Bottom row is a higher magnification of the boxed areas. Scale bar, 10 μm.

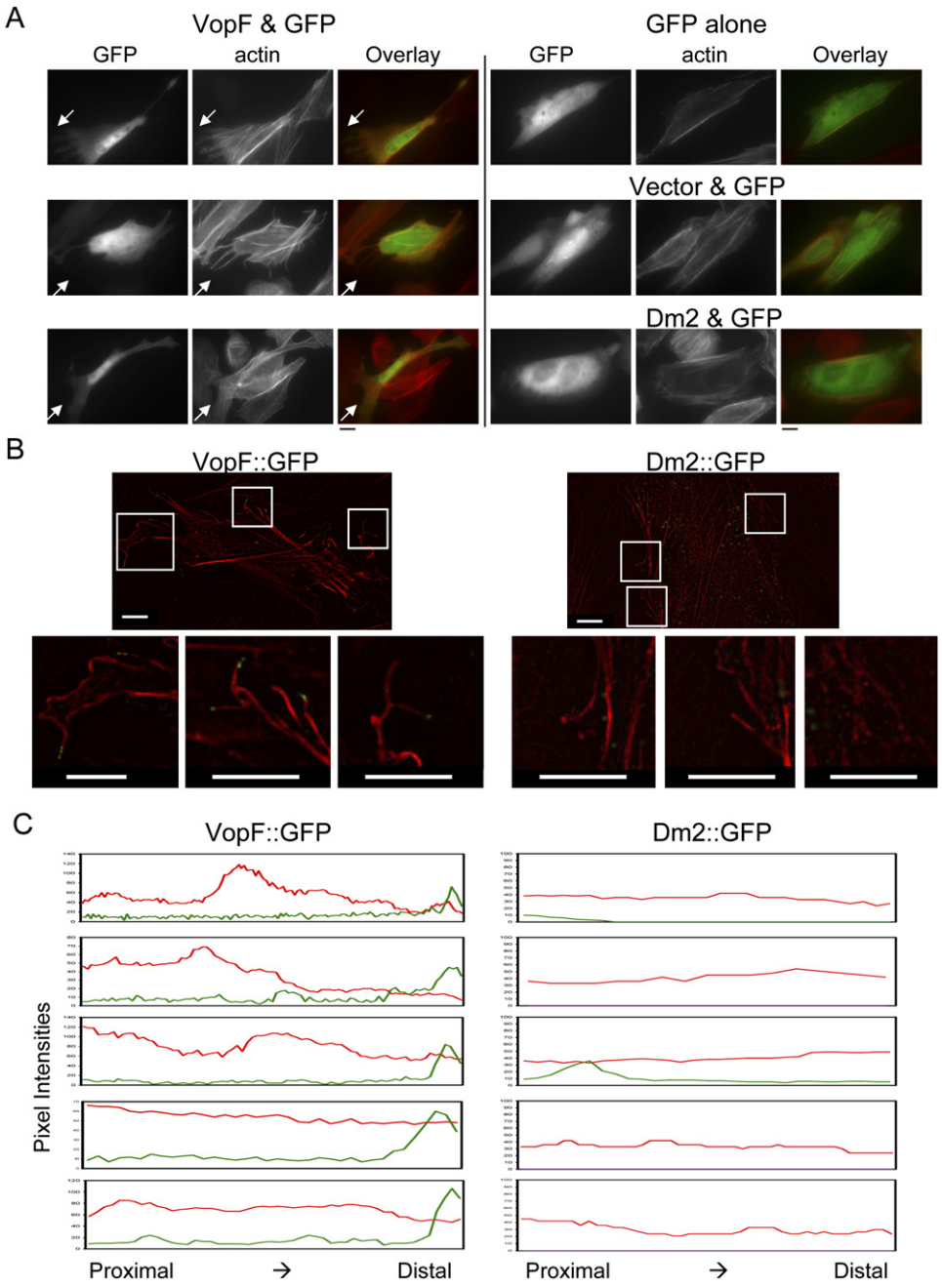

Figure 6. Transfection of VopF Is Sufficient to Induce Actin-Rich Filoform Formation

(A) CHO cells were transfected with *vopF*::pCMV-HA and Dm2::pCMV-HA. pAcGFP-N1 was cotransfected as a control for cells that had taken up the plasmid DNA. Twenty-four hours posttransfection, cells were fixed and permeabilized as described above and stained for actin using Texas red phalloidin (red). White arrows point to the aberrant protrusions from the transfected cells.

(B) CHO cells were transfected with *vopF*::pAcGFP-N1 or Dm2::pAcGFP-N1 to express VopF-GFP or Dm2-GFP fusion proteins. Micrographs were processed for 2D deconvolution. Overlay images of Texas red phalloidin (red) and VopF-GFP or Dm2-GFP (green) were shown. Bottom row is higher magnification of the boxed areas. Scale bar, 10 μm.

(C) Line scan measurements of pixel intensities for actin-rich filoform protrusions. x axis showed the position of the protrusions from proximal to distal ends. y axis showed pixel intensities. Red lines denote pixel intensities of actin (Texas red phalloidin). Green lines denote pixel intensities of VopF-GFP or Dm2-GFP. Five representative line scans were shown for protrusions from five VopF::GFP- or Dm2::GFP-transfected cells.

Neutrophils are recruited to the site of infection by chemotaxis to kill pathogens via endocytosis; both of these processes require the actin cytoskeleton.

VopF belongs to a new group of bacterial virulence factors that directly nucleate or modulate actin filaments. Other virulence factors in this group include the TARP

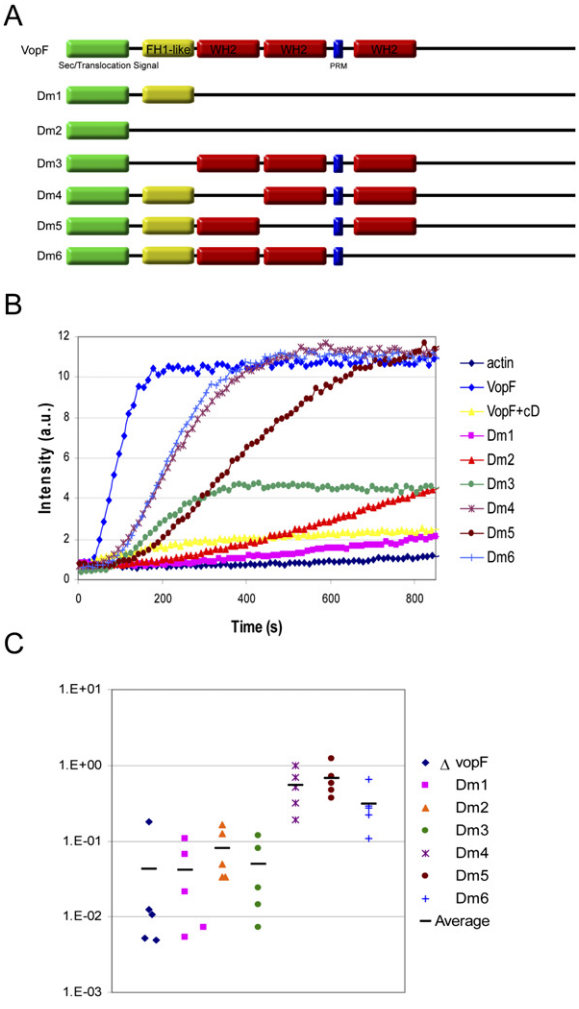

Figure 7. Domain Analysis of VopF Activity In Vitro and In Vivo

(A) Domain deletion mutants of VopF. VopF mutant 1 (Dm1) has all three WH2 domains deleted. Dm2 has a deletion in FH1-like and all three WH2 domains. Dm3 has a deletion in the FH1-like domain. Dm4, 5, and 6 each have a deletion in one of the three different WH2 domains.

(B) Pyrene actin assay of VopF and deletion mutants. VopF or mutant protein (100 nM) was incubated with 2 μM monomeric pyrene-labeled actin. Actin polymerization was measured as arbitrary fluorescence intensity (Intensity a.u.) over time (seconds) with excitation and emission wavelengths of 365 and 407 nm, respectively. A mixture of actin and pyrene actin, labeled as actin alone, served as a negative control. Cytochalasin D (cD) (2 μM), which blocks barbed-end polymerization, was used as an inhibitor.

(C) Competitive indexes of VopF deletion mutants against AM-19226 in the infant mouse model. Competitive index is calculated as the ratio of output of test strain:reference strain over the ratio of input of test strain:reference strain.

protein from *Chlamydia*, which has one WH2 domain and nucleates actin as an oligomer (Jewett et al., 2006), SipC from *Salmonella* (Hayward and Koronakis, 2002), and IpaC from *Shigella* (Tran Van Nhieu et al., 1999), which have both actin nucleating and bundling activities. With no homology to any known actin-binding domain, SipC has been proposed as a functional mimic of the Arp2/3 complex (Hayward and Koronakis, 2002).

While bacterial pathogens have evolved multiple mechanisms to manipulate the Arp2/3 pathway in nucleating actin, molecular mimicry of formin (FH1 and FH2 domains) or Spire (four WH2 domains) has not been reported previously. This study demonstrates that VopF mimics formin activity using domains homologous to both formin and Spire. Our domain deletion analysis (Figure 6) suggests that both FH1-like and WH2 domains of VopF are required for actin nucleation and polymerization activity as well as efficient colonization by *V. cholerae* AM-19226 of the mouse small intestine. Based on its localization at the fast-growing barbed end of the actin-rich protrusions, we believe that VopF may function more like formin than Spire. Formin is involved in the actin-driven processes of cell polarity, cytokinesis, cell motility, and endocytosis (Faix and Grosse, 2006). By mimicking formin, VopF may target host epithelial cells and alter actin-dependent properties such as tight junctional integrity, vesicular trafficking, distribution of receptors on their surface, or brush border membrane formation (Mitic and Anderson, 1998; Stamnes, 2002; Jesaitis and Klotz, 1993; Hofer et al., 1998; Fath et al., 1993).

Interestingly, the intestinal surface is lined with polarized epithelial cells, and one of the functions of formin is to maintain cell polarity (Feierbach and Chang, 2001). Delivery of VopF into the epithelial cells may disrupt the homeostasis of cell polarity and affect the formation or function of the brush border in a way that stimulates bacterial adherence or survival in this microenvironment.

In other T3SS, effectors have been discovered to target cytokinesis and block epithelial wound repair (Shafikhani and Engel, 2006). VopF may disrupt cytokinesis by mimicking formin and interfering with cellular processes such as repair of intestinal lesions caused by other toxins such as RtxA and HlyA (Fullner and Mekalanos, 2000; Mitra et al., 2000). These hypothetical effects of VopF will require extensive cell biological and histological examination of the VopF-dependent, AM-19226-host epithelium interaction.

We have shown that a functional T3SS in *V. cholerae* AM-19226 is required for intestinal colonization in the infant mouse model and that the T3SS effector protein VopF is necessary for this virulence-related phenotype. VopF alters actin polymerization in vitro as well as the structure of the host cell cytoskeleton. These two effects, which disrupt actin homeostasis, correlate with the requirement of VopF for efficient intestinal colonization. As a functional mimic of formin, VopF, a domain hybrid between formin and Spire, provides a novel virulence mechanism as well as a valuable tool for studying cell biological processes involving the actin cytoskeleton.

EXPERIMENTAL PROCEDURES

Cell Line and Bacterial Strains

Human epithelial HEp-2 cells (ATCC CCL-23) were cultivated in RPMI supplemented with 10% fetal calf serum (FCS), L-glutamine (2 mM), and penicillin/streptomycin at 37°C in a 5% CO_2 atmosphere. CHO cells (ATCC CCL-61) were cultivated in Ham's F12K medium

supplemented with 10% FCS, L-glutamine (2 mM) adjusted to contain 1.5 g/l sodium bicarbonate.

V. cholerae AM-19226, a non-O1, non-O139 strain of serogroup O39 and N16961, an O1 El Tor biotype, were used in this study. *E. coli* and *V. cholerae* strains were propagated in LB containing appropriate antibiotics at 37°C.

Strain Construction

Strains and plasmids are listed in Table S1 in the Supplemental Data available with this article online. Mutations in *vcsN2*, *vcsC2*, and *vcsJ2* were constructed by marker exchange mutagenesis in which the entire open reading frame was replaced by a kanamycin resistance cassette (Mekalanos et al., 1983). Other mutations were constructed by in-frame deletions of the entire reading frame and have been described previously (Skorupski and Taylor, 1996).

Southern Analysis

Southern hybridization analysis was performed as previously described (Dziejman et al., 2005). The *vopF* probe was obtained by PCR amplification using AM-19226 genomic DNA as template.

Translocation Assay

Translocation assays were performed as described previously (Charpentier and Oswald, 2004). *blaM* gene (encoding TEM-1) was cloned into pDSW204 to generate pVTM30. Genes encoding VopF (full-length 1–530 aa), VopF (1–100 aa), and Vpa1346 (full-length 1–289 aa) were cloned into pVTM30 to generate pVTM305, pVTM32, and pVTM31, respectively.

HEp-2 cells were seeded at 5×10^4 cells per well in Labtek 8-well chamber slides (Becton Dickinson) in 500 μl of RPMI. Bacteria were inoculated in LB with streptomycin/ampicillin. On the following day, bacteria were subcultured 1:100 in LB with streptomycin/ampicillin and IPTG (0.8 mM) and grown at 37°C for 2 hr. HEp-2 cells were washed and infected with 10^5 bacteria for 3 hr. CCF2/AM was added for 1 hr. Slides were covered with coverslips and observed using a Zeiss inverted fluorescence microscope.

Western Blot Analysis of TEM-1 Fusion Proteins

Cells were grown to log phase in the presence or absence of IPTG. Cell extracts were subjected to SDS/PAGE, transferred to nitrocellulose membrane, probed with anti-β lactamase antibody (Chemicon), and visualized by Supersignal western blotting kit (Pierce).

Polyclonal Antibodies against AM-19226 and VopF

AM-19226 was grown in LB medium to stationary phase, and cfu were determined by plating serial dilutions of the culture. Bacterial cells were heat inactivated at 56°C for 1 hr, pelleted, and resuspended in PBS. To prepare anti-AM-19226 antibodies, 10^6 CFU were used to immunize a New Zealand white rabbit (Covance). Purified VopF protein was used as immunogen to produce polyclonal antibodies in rabbit (Cocalico Biologicals, Inc).

Infant Mouse Colonization

Infant mouse colonization assay was described previously (Gardel and Mekalanos, 1996). *V. cholerae* (10^6) were inoculated intragastrically into 5-day-old CD-1 mice (Charles River Laboratories). Infected pups were killed after 20 hr, and intestinal colonized bacteria were quantified as described previously (Gardel and Mekalanos, 1996). Competition assay was performed by coinoculating with AM-19226 (ΔlacZ). Differentiation of wild-type or mutant strains was based on blue/white colonies on LB plates containing X-gal. Competitive index was calculated as the ratio of CFU of test strain:CFU of reference strain/the ratio of inoculum of test strain:inoculum of reference strain. If no CFU were recovered from the intestine, a colony of one was assigned to the lowest dilution.

Protein Expression and Purification

vopF and *vopF* mutant genes were cloned into pET28a (EMD Biosciences), which introduces an N-terminal fusion of the protein to a His6-tag. BL21(DE3) strains carrying expression plasmids were subcultured 1:1000 into 1 l 2× YT medium growing at 37°C with aeration until optical density at 600 nm reached 0.5 and were induced using 0.8 mM IPTG and incubated at 18°C overnight. Cells were harvested; suspended in 500 mM NaCl, 50 mM Tris (pH 7.5), 10% glycerol, 15 mM imidazole, and 2 mM β-mercaptoethanol; and lysed by lysozyme and sonication. The fusion protein was purified by affinity chromatography using His-Trap HP (GE Health Systems).

Pyrene Actin Assay

Pyrene actin assay was described previously (Ho et al., 2006). Rabbit skeletal muscle actin (Brieher et al., 2004) was purified as described previously. Protein samples were dialyzed using Slide-a-lyzer (Pierce) in assay buffer for 2 hr, and 100 nM of VopF or mutant protein was used in the assays unless specified.

HEp-2 Infection

HEp-2 cells were seeded in Labtek 4-well chamber slides at 2×10^5 cells per well. On the next day, *V. cholerae* strains were subcultured to log phase in LB at 37°C. A MOI of 3 was used to infect the HEp-2 cells, which were fixed 3 hr later using 3.7% formaldehyde. Cells were permeabilized using 0.1% Triton X-100. Rabbit anti-AM-19226 antibodies, rabbit anti-VopF antibodies, and Alexa Fluor 568 goat anti-rabbit antibodies (Invitrogen) were used to visualize the bacteria or VopF protein. Alexa Fluor 488 phalloidin and DAPI (Invitrogen) were used to stain the actin and nucleus, respectively. The slides were then covered with coverslips and observed on a Zeiss inverted fluorescence microscope.

CHO Cell Transfection

vopF and Dm2 (*vopF*ΔFH1L 3WH2) genes were cloned into pCMV-HA (Clontech) and pAcGFP-N1 (Clontech) to make transfection vectors expressing amino terminus HA tagged and GFP fusion proteins, respectively. pAcGFP-N1 (Clontech), which encodes a GFP from *Aequorea coerulescens*, was also used as a positive control for transfection. Plasmid DNA was extracted using Endo-free Maxiprep (Qiagen).

CHO cells were seeded in Labtek 8-well chamber slides. jetPEI (polyPlus) transfection reagent was used as recommended by manufacturer. Twenty-four hours posttransfection, cells were fixed with 3.7% formaldehyde and permeabilized with 0.1% Triton X-100. Actin filaments were stained with Alexa Fluor 568 phalloidin (Invitrogen). The slides were then covered with coverslips and observed on a Zeiss inverted fluorescence microscope.

Supplemental Data

The Supplemental Data include a supplemental table of all bacterial strains and plasmids used in this study and can be found with this article online at http://www.cellhostandmicrobe.com/cgi/content/full/1/2/95/DC1/.

ACKNOWLEDGMENTS

We thank Vincent Lee for the *blaM* construct and helpful advice and Andres Lebensohn and Marc Kirschner for use of a fluorescence spectrometer. We also thank Emily Pierson and Elizabeth Shakhnovich for critical reading of the manuscript; Hao Yuan Kueh and members of the Mekalanos lab for helpful discussions. This work was supported by National Institutes of Health Grant AI18045 and by AI026289. V.C.T. was supported by NSF predoctoral fellowship.

Received: January 16, 2007
Revised: March 1, 2007
Accepted: March 22, 2007
Published: April 18, 2007

REFERENCES

Aragon, V., Chao, K., and Dreyfus, L.A. (1997). Effect of cytolethal distending toxin on F-actin assembly and cell division in Chinese hamster ovary cells. Infect. Immun. *65*, 3774–3780.

Brieher, W.M., Coughlin, M., and Mitchison, T.J. (2004). Fascin-mediated propulsion of Listeria monocytogenes independent of frequent nucleation by the Arp2/3 complex. J. Cell Biol. *165*, 233–242.

Campellone, K.G., Giese, A., Tipper, D.J., and Leong, J.M. (2002). A tyrosine-phosphorylated 12-amino-acid sequence of enteropathogenic Escherichia coli Tir binds the host adaptor protein Nck and is required for Nck localization to actin pedestals. Mol. Microbiol. *43*, 1227–1241.

Charpentier, X., and Oswald, E. (2004). Identification of the secretion and translocation domain of the enteropathogenic and enterohemorrhagic Escherichia coli effector Cif, using TEM-1 beta-lactamase as a new fluorescence-based reporter. J. Bacteriol. *186*, 5486–5495.

Collazo, C.M., and Galan, J.E. (1997). The invasion-associated type-III protein secretion system in Salmonella—A review. Gene *192*, 51–59.

Cossart, P. (1997). Host/pathogen interactions. Subversion of the mammalian cell cytoskeleton by invasive bacteria. J. Clin. Invest. *99*, 2307–2311.

Cossart, P. (2000). Actin-based motility of pathogens: The Arp2/3 complex is a central player. Cell. Microbiol. *2*, 195–205.

Dziejman, M., Serruto, D., Tam, V.C., Sturtevant, D., Diraphat, P., Faruque, S.M., Rahman, M.H., Heidelberg, J.F., Decker, J., Li, L., et al. (2005). Genomic characterization of non-O1, non-O139 Vibrio cholerae reveals genes for a type III secretion system. Proc. Natl. Acad. Sci. USA *102*, 3465–3470.

Evangelista, M., Pruyne, D., Amberg, D.C., Boone, C., and Bretscher, A. (2002). Formins direct Arp2/3-independent actin filament assembly to polarize cell growth in yeast. Nat. Cell Biol. *4*, 260–269.

Faix, J., and Grosse, R. (2006). Staying in shape with formins. Dev. Cell *10*, 693–706.

Faruque, S.M., Albert, M.J., and Mekalanos, J.J. (1998). Epidemiology, genetics, and ecology of toxigenic Vibrio cholerae. Microbiol. Mol. Biol. Rev. *62*, 1301–1314.

Faruque, S.M., Chowdhury, N., Kamruzzaman, M., Dziejman, M., Rahman, M.H., Sack, D.A., Nair, G.B., and Mekalanos, J.J. (2004). Genetic diversity and virulence potential of environmental Vibrio cholerae population in a cholera-endemic area. Proc. Natl. Acad. Sci. USA *101*, 2123–2128.

Fath, K.R., Mamajiwalla, S.N., and Burgess, D.R. (1993). The cytoskeleton in development of epithelial cell polarity. J. Cell Sci. Suppl. *17*, 65–73.

Feierbach, B., and Chang, F. (2001). Roles of the fission yeast formin for3p in cell polarity, actin cable formation and symmetric cell division. Curr. Biol. *11*, 1656–1665.

Fiorentini, C., Falzano, L., Travaglione, S., and Fabbri, A. (2003). Hijacking Rho GTPases by protein toxins and apoptosis: Molecular strategies of pathogenic bacteria. Cell Death Differ. *10*, 147–152.

Fullner, K.J., and Mekalanos, J.J. (2000). In vivo covalent cross-linking of cellular actin by the Vibrio cholerae RTX toxin. EMBO J. *19*, 5315–5323.

Fullner, K.J., Boucher, J.C., Hanes, M.A., Haines, G.K., III, Meehan, B.M., Walchle, C., Sansonetti, P.J., and Mekalanos, J.J. (2002). The contribution of accessory toxins of Vibrio cholerae O1 El Tor to the proinflammatory response in a murine pulmonary cholera model. J. Exp. Med. *195*, 1455–1462.

Galan, J.E., and Collmer, A. (1999). Type III secretion machines: Bacterial devices for protein delivery into host cells. Science *284*, 1322–1328.

Galan, J.E., and Wolf-Watz, H. (2006). Protein delivery into eukaryotic cells by type III secretion machines. Nature *444*, 567–573.

Gardel, C.L., and Mekalanos, J.J. (1996). Alterations in Vibrio cholerae motility phenotypes correlate with changes in virulence factor expression. Infect. Immun. *64*, 2246–2255.

Goldberg, M.B. (2001). Actin-based motility of intracellular microbial pathogens. Microbiol. Mol. Biol. Rev. *65*, 595–626.

Goldberg, M.B., and Theriot, J.A. (1995). Shigella flexneri surface protein IcsA is sufficient to direct actin-based motility. Proc. Natl. Acad. Sci. USA *92*, 6572–6576.

Goosney, D.L., DeVinney, R., and Finlay, B.B. (2001). Recruitment of cytoskeletal and signaling proteins to enteropathogenic and enterohemorrhagic Escherichia coli pedestals. Infect. Immun. *69*, 3315–3322.

Hayward, R.D., and Koronakis, V. (2002). Direct modulation of the host cell cytoskeleton by Salmonella actin-binding proteins. Trends Cell Biol. *12*, 15–20.

Higgs, H.N. (2005). Formin proteins: A domain-based approach. Trends Biochem. Sci. *30*, 342–353.

Ho, H.Y., Rohatgi, R., Lebensohn, A.M., and Kirschner, M.W. (2006). In vitro reconstitution of cdc42-mediated actin assembly using purified components. Methods Enzymol. *406*, 174–190.

Hofer, D., Jons, T., Kraemer, J., and Drenckhahn, D. (1998). From cytoskeleton to polarity and chemoreception in the gut epithelium. Ann. N Y Acad. Sci. *859*, 75–84.

Hueck, C.J. (1998). Type III protein secretion systems in bacterial pathogens of animals and plants. Microbiol. Mol. Biol. Rev. *62*, 379–433.

Isberg, R.R., and Van Nhieu, G.T. (1994). Two mammalian cell internalization strategies used by pathogenic bacteria. Annu. Rev. Genet. *28*, 395–422.

Jesaitis, A.J., and Klotz, K.N. (1993). Cytoskeletal regulation of chemotactic receptors: Molecular complexation of N-formyl peptide receptors with G proteins and actin. Eur. J. Haematol. *51*, 288–293.

Jewett, T.J., Fischer, E.R., Mead, D.J., and Hackstadt, T. (2006). Chlamydial TARP is a bacterial nucleator of actin. Proc. Natl. Acad. Sci. USA *103*, 15599–15604.

Kitayama, C., and Uyeda, T.Q. (2003). ForC, a novel type of formin family protein lacking an FH1 domain, is involved in multicellular development in Dictyostelium discoideum. J. Cell Sci. *116*, 711–723.

Kovach, M.E., Elzer, P.H., Hill, D.S., Robertson, G.T., Farris, M.A., Roop, R.M., II, and Peterson, K.M. (1995). Four new derivatives of the broad-host-range cloning vector pBBR1MCS, carrying different antibiotic-resistance cassettes. Gene *166*, 175–176.

Kovar, D.R., Kuhn, J.R., Tichy, A.L., and Pollard, T.D. (2003). The fission yeast cytokinesis formin Cdc12p is a barbed end actin filament capping protein gated by profilin. J. Cell Biol. *161*, 875–887.

Lerm, M., Schmidt, G., and Aktories, K. (2000). Bacterial protein toxins targeting rho GTPases. FEMS Microbiol. Lett. *188*, 1–6.

Machesky, L.M., Insall, R.H., and Volkman, L.E. (2001). WASP homology sequences in baculoviruses. Trends Cell Biol. *11*, 286–287.

Mekalanos, J.J., Swartz, D.J., Pearson, G.D., Harford, N., Groyne, F., and de Wilde, M. (1983). Cholera toxin genes: Nucleotide sequence, deletion analysis and vaccine development. Nature *306*, 551–557.

Mitic, L.L., and Anderson, J.M. (1998). Molecular architecture of tight junctions. Annu. Rev. Physiol. *60*, 121–142.

Mitra, R., Figueroa, P., Mukhopadhyay, A.K., Shimada, T., Takeda, Y., Berg, D.E., and Nair, G.B. (2000). Cell vacuolation, a manifestation of the El tor hemolysin of Vibrio cholerae. Infect. Immun. *68*, 1928–1933.

Moseley, J.B., Sagot, I., Manning, A.L., Xu, Y., Eck, M.J., Pellman, D., and Goode, B.L. (2004). A conserved mechanism for Bni1- and mDia1-induced actin assembly and dual regulation of Bni1 by Bud6 and profilin. Mol. Biol. Cell *15*, 896–907.

Park, K.S., Ono, T., Rokuda, M., Jang, M.H., Okada, K., Iida, T., and Honda, T. (2004). Functional characterization of two type III secretion systems of Vibrio parahaemolyticus. Infect. Immun. *72*, 6659–6665.

Paunola, E., Mattila, P.K., and Lappalainen, P. (2002). WH2 domain: A small, versatile adapter for actin monomers. FEBS Lett. *513*, 92–97.

Pellegrin, S., and Mellor, H. (2005). The Rho family GTPase Rif induces filopodia through mDia2. Curr. Biol. *15*, 129–133.

Peng, J., Wallar, B.J., Flanders, A., Swiatek, P.J., and Alberts, A.S. (2003). Disruption of the Diaphanous-related formin Drf1 gene encoding mDia1 reveals a role for Drf3 as an effector for Cdc42. Curr. Biol. *13*, 534–545.

Peterson, K.M., and Mekalanos, J.J. (1988). Characterization of the Vibrio cholerae ToxR regulon: Identification of novel genes involved in intestinal colonization. Infect. Immun. *56*, 2822–2829.

Petrella, E.C., Machesky, L.M., Kaiser, D.A., and Pollard, T.D. (1996). Structural requirements and thermodynamics of the interaction of proline peptides with profilin. Biochemistry *35*, 16535–16543.

Pierce, N.F., Kaper, J.B., Mekalanos, J.J., and Cray, W.C., Jr. (1985). Role of cholera toxin in enteric colonization by Vibrio cholerae O1 in rabbits. Infect. Immun. *50*, 813–816.

Popoff, M.R. (1998). Interactions between bacterial toxins and intestinal cells. Toxicon *36*, 665–685.

Pruyne, D., Evangelista, M., Yang, C., Bi, E., Zigmond, S., Bretscher, A., and Boone, C. (2002). Role of formins in actin assembly: Nucleation and barbed-end association. Science *297*, 612–615.

Quinlan, M.E., Heuser, J.E., Kerkhoff, E., and Mullins, R.D. (2005). Drosophila Spire is an actin nucleation factor. Nature *433*, 382–388.

Rivero, F., Muramoto, T., Meyer, A.K., Urushihara, H., Uyeda, T.Q., and Kitayama, C. (2005). A comparative sequence analysis reveals a common GBD/FH3–FH1-FH2-DAD architecture in formins from Dictyostelium, fungi and metazoa. BMC Genomics *6*, 28.

Rottner, K., Stradal, T.E., and Wehland, J. (2005). Bacteria-host-cell interactions at the plasma membrane: Stories on actin cytoskeleton subversion. Dev. Cell *9*, 3–17.

Schirenbeck, A., Bretschneider, T., Arasada, R., Schleicher, M., and Faix, J. (2005). The Diaphanous-related formin dDia2 is required for the formation and maintenance of filopodia. Nat. Cell Biol. *7*, 619–625.

Shafikhani, S.H., and Engel, J. (2006). Pseudomonas aeruginosa type III-secreted toxin ExoT inhibits host-cell division by targeting cytokinesis at multiple steps. Proc. Natl. Acad. Sci. USA *103*, 15605–15610.

Skorupski, K., and Taylor, R.K. (1996). Positive selection vectors for allelic exchange. Gene *169*, 47–52.

Smith, G.A., and Portnoy, D.A. (1997). How the Listeria monocytogenes ActA protein converts actin polymerization into a motile force. Trends Microbiol. *5*, 272–276.

Stamnes, M. (2002). Regulating the actin cytoskeleton during vesicular transport. Curr. Opin. Cell Biol. *14*, 428–433.

Stevens, J.M., Galyov, E.E., and Stevens, M.P. (2006). Actin-dependent movement of bacterial pathogens. Nat. Rev. Microbiol. *4*, 91–101.

Thelin, K.H., and Taylor, R.K. (1996). Toxin-coregulated pilus, but not mannose-sensitive hemagglutinin, is required for colonization by Vibrio cholerae O1 El Tor biotype and O139 strains. Infect. Immun. *64*, 2853–2856.

Tran Van Nhieu, G., Caron, E., Hall, A., and Sansonetti, P.J. (1999). IpaC induces actin polymerization and filopodia formation during Shigella entry into epithelial cells. EMBO J. *18*, 3249–3262.

Welch, M.D., Rosenblatt, J., Skoble, J., Portnoy, D.A., and Mitchison, T.J. (1998). Interaction of human Arp2/3 complex and the Listeria monocytogenes ActA protein in actin filament nucleation. Science *281*, 105–108.